

PFC/RR-91-14

DOE/ET-51013-295

**SAFETY AND PROTECTION FOR LARGE-SCALE
MAGNET SYSTEMS – FY91 REPORT**

R.J. Thome, B.A. Smith and A. Shajii

February 1992

Plasma Fusion Center
Massachusetts Institute of Technology
Cambridge, Massachusetts 02139

Submitted to
Idaho National Engineering Laboratory
Idaho Falls, Idaho

This work was supported in part by EG&G Subcontract # C88-110982-TKP-154-87

Table of Contents

| | Page No. |
|---|----------|
| 1.0 Introduction and Summary | 1 |
| 1.1 Magnet Failure Incidents | 1 |
| 1.2 Quench Code Development | 2 |
| 2.0 Magnet Failure Incidents | 3 |
| 2.1 CDIF MHD Magnet | 3 |
| 2.1.1 Magnet Design and Operation | 3 |
| 2.1.2 Failure Discovery | 6 |
| 2.1.3 Other Items Noted During Evaluation | 8 |
| 2.1.4 Recommendations from Evaluation | 8 |
| 2.1.5 Present Magnet Status | 11 |
| 2.2 TEXT Tokamak | 11 |
| 2.2.1 Coil Design | 11 |
| 2.2.2 Failure Discovery | 14 |
| 2.2.3 Failure Evaluation | 14 |
| 2.2.4 Recommendations from Evaluation | 16 |
| 2.2.5 Present Coil Status | 16 |
| 2.3 ATF Stellarator | 17 |
| 2.3.1 Coil Design | 17 |
| 2.3.2 Failure Discovery | 17 |
| 2.3.3 Failure Evaluation | 17 |
| 2.3.4 Recommendations from Evaluation | 20 |
| 2.3.5 Present Magnet Status | 20 |
| 3.0 Quench Code Development | 22 |
| 3.1 HESTAB & CICC Capabilities | 22 |
| 3.2 Comparison with Bus Data | 24 |
| 3.3 Future Work | 24 |

**MIT Plasma Fusion Center
FY91 Safety and Protection Annual Report**

1.0 Introduction and Summary

1.1 Magnet Failure Incidents

During FY91, there were three notable failures of conventional, water-cooled copper magnets investigated with partial support from this program. The first was at the CDIF MHD facility in Butte, MT, the second at the TEXT tokamak at the University of Texas at Austin, and the third at the ATF tokamak located at Oak Ridge, TN. In each case the failed coils were inspected, the circumstances surrounding the failures were reviewed, and suggestions for improving magnet reliability in the future were made.

The CDIF iron core magnet completed fabrication in 1980 and was acceptance tested in 1981. It has been operated successfully for 10 years by Montana State Energy Inc.(MSE) until the recent failure in February 1991.

The magnet consists of two symmetrical saddle-magnet halves. Each half contains 15 tons of water-cooled, hollow copper conductor which is insulated, epoxy impregnated, and embedded in a 70 ton iron return frame. There are six double pancake coil windings and 52 independent water cooling paths fed via flexible hoses from a common manifold for each magnet half. The flexible hoses feed copper tubes which enter the coil winding cross section in the end-turn region of the saddle at the MHD-outlet end of the magnet. The end turns are spread to provide spacing for the tubing between the coil double pancakes. The tubes are brazed to custom-machined, right-angle fittings, which are, in turn, brazed to the winding.

On the day of the magnet failure, a problem with the MHD channel had caused an emergency shutdown. Prior to parting the magnet at the midplane to access the channel, the magnet crossover bus bar was grounded as a safety precaution. When the bus bar was grounded, a control power fuse blew, indicating the presence of control power on the magnet, which is abnormal. After substantial evaluation and analysis it was concluded that a failure occurred in one of the right angle fittings, causing water to leak into the surrounding insulation. Ultimately, the lead was repaired with a metal sealant and a resumption of operations was attempted after ten months of down time.

The Texas Experimental Tokamak (TEXT) upgrade machine is a medium-sized tokamak which was upgraded to a 1.05 m major radius with a new vacuum vessel and a new poloidal field coil set to study diverted and H-mode plasma configurations [1]. The poloidal coil set includes vertical field (VF), ohmic heating (OH) and divertor (DIV) windings, all shaped as rings and located inside the bore of the toroidal field (TF) coil, between the vacuum vessel and the TF conductor. There are three divertor windings, designated as upper, middle and lower, and each

of these windings are divided into two bundles, a divertor and a bias bundle. The ring coils are built as two 180° segments. The turns are joined by short removable jumpers which have fingers which mate to the coil turn ends. Mating surfaces are plated and clamped to provide electrical continuity at the joint.

During the initial plasma operations, following an increase in the plasma current from 150-175 kA to 200 kA, the plasma became very disruptive and the sound of the shots changed. Subsequent investigation showed flashover had occurred inside the lower divertor winding, between the bias and divertor winding bundles. A new design using welded joints has been proposed for replacement coils in lieu of attempting repair.

The Advanced Toroidal Facility (ATF) is a stellarator fusion device which was designed and constructed during the mid to late 1980's at Oak Ridge National Laboratory [2]. The design of the helical field (HF) coils was unique in that these coils comprised multiple, identical segments, each making a bolted joint to the next at the horizontal midplane. This configuration enabled the HF coils and the vacuum vessel manufacture and assembly to proceed in parallel. The machine had operated for nearly 20,000 shots with over 2,000 of these near the design point of 2 tesla.

In May of 1991, the first 2 tesla shot was fired since a single 2 tesla shot had been fired two months earlier. The HF power supply was turned on and applied normal voltage to the HF coils. The outer and inner vertical field coils were then powered in sequence. At that time a loud shotgun-like sound was heard throughout the facility, and the operator observed arcing on the TV monitor [3]. Upon disassembly, there were indications of several turn-to-turn faults within one of the HF coil segments, and severe damage to at least two of the 24 segments was sustained. A temporary repair involving cleanup and epoxy-based insulating paint enabled a return to operation at reduced duty cycle. Final repair requires a complete machine disassembly which is underway now.

Included in this report are summaries of the findings for each of the magnet failures and the suggestions for improving magnet reliability in the future.

1.2 Quench Code Development

In FY91, we continued evaluation of two codes (HESTAB and CICC) for possible modification for quench and protection analyses. The codes were tested against data taken at MIT on simulated bus for the SSCL dipole magnets. Both codes were found to predict energy margin reasonably well. This is the amount of energy required as local input to initiate a propagating normal zone. However, analysis of the characteristics of the zone while propagating was not within the scope of HESTAB and data correlation using CICC was poor. Results are outlined in this report and modifications to improve speed as well as predictive capability will continue in FY92.

2.0 Magnet Failure Incidents

2.1 CDIF MHD Magnet

2.1.1 Magnet Design and Operation

The CDIF iron core magnet has water-cooled copper windings and a pole set and return frame made from carbon steel. The magnet assembly weighs approximately 170 tons. An artist's drawing of the magnet is shown in Figure 1. The magnet is built in symmetrical halves which part on rollers at the midplane to provide access to the MHD channel located in the magnet bore. A crossover bus bar connects the two magnet halves electrically. The magnet produces a peak field on the MHD channel axis of 3 T at a nominal operating current of about 8300 A. The saddle winding in each magnet half contains 144 turns in a 12 x 12 bundle arrangement, with 6 double pancake coils of 24 turns each. A cross section of the hollow copper conductor is shown in Figure 2. Separate feed and return manifolds provide flow through hoses and tubing to 52 individual water cooling paths per magnet half. Flow paths are two turns each in the outer (longer turn) region of the winding, and 3 turns each in the inner (shorter turn) region of the winding. Each cooling hose is connected to a copper tube which is brazed to a right angle fitting, as shown in Figure 3, in the MHD-outlet end-turn region of the saddles. The axially directed electromagnetic loads on each saddle end are reacted by a set of 8, 1-1/2" diameter, high strength, 1141 steel tie rods.

The magnet was specifically designed for operation at a constant average conductor temperature of 60° C to minimize the thermal contribution to the winding stresses. Prior to the first magnet operation, the windings were preheated to 60° C and then the tie-rod nuts and jam nuts were run-in to the end plates. This established a zero-axial-load-at-temperature condition, prior to energization of the magnet. Upon energization, as the electromagnetic load is applied, the tie rods react only this load component, since the average temperature of the windings is controlled to be constant during operation. This is accomplished with a flow controller, which regulates the flow as a function of current to keep the magnet average temperature constant. The magnet operated successfully with this scenario for ten years with 240 full-field cycles.

Each of the winding cooling paths has a temperature switch which provides a control signal to shut the magnet down on an over-temperature condition. The switch opens on increasing temperature. Over the years, contacts of some of the temperature switches have become shorted to the magnet turns on which they are mounted. When this happens, not only does switch status become unreliable, but also 120 Vac control power is shorted to the magnet, creating a safety hazard for service. As the contact shortings have occurred and have been discovered, these contacts are taken off the 120 Vac control power circuit and placed in a battery driven, 3 Vdc circuit which provides LED indication of contact closure at a status panel. During magnet operation, an operator is located at the temperature switch status panel, and, if an LED is extinguished during a run, the operator is obligated to communicate the need for an emergency shutdown of the magnet. Rampdown takes 10-11 seconds.

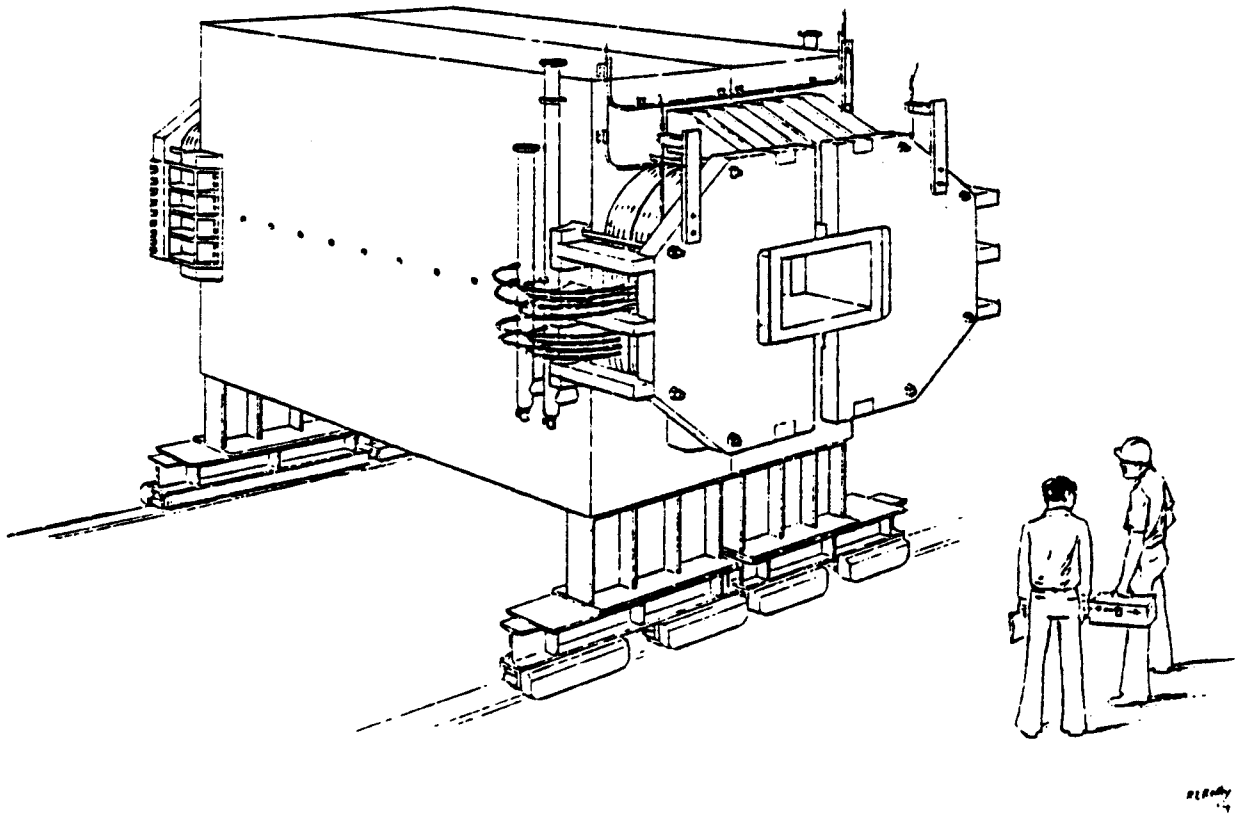


Figure 1 Artist's Drawing of CDIF Conventional Magnet (from Ref. 5)

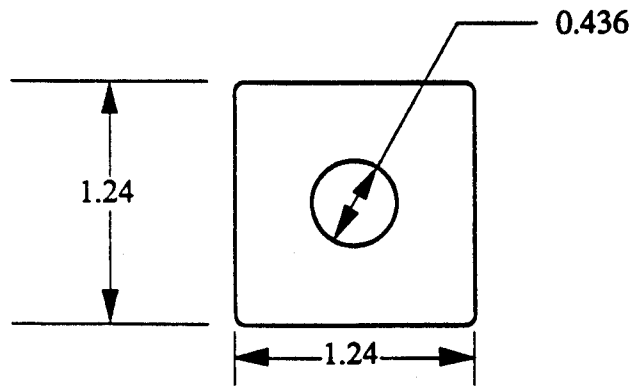
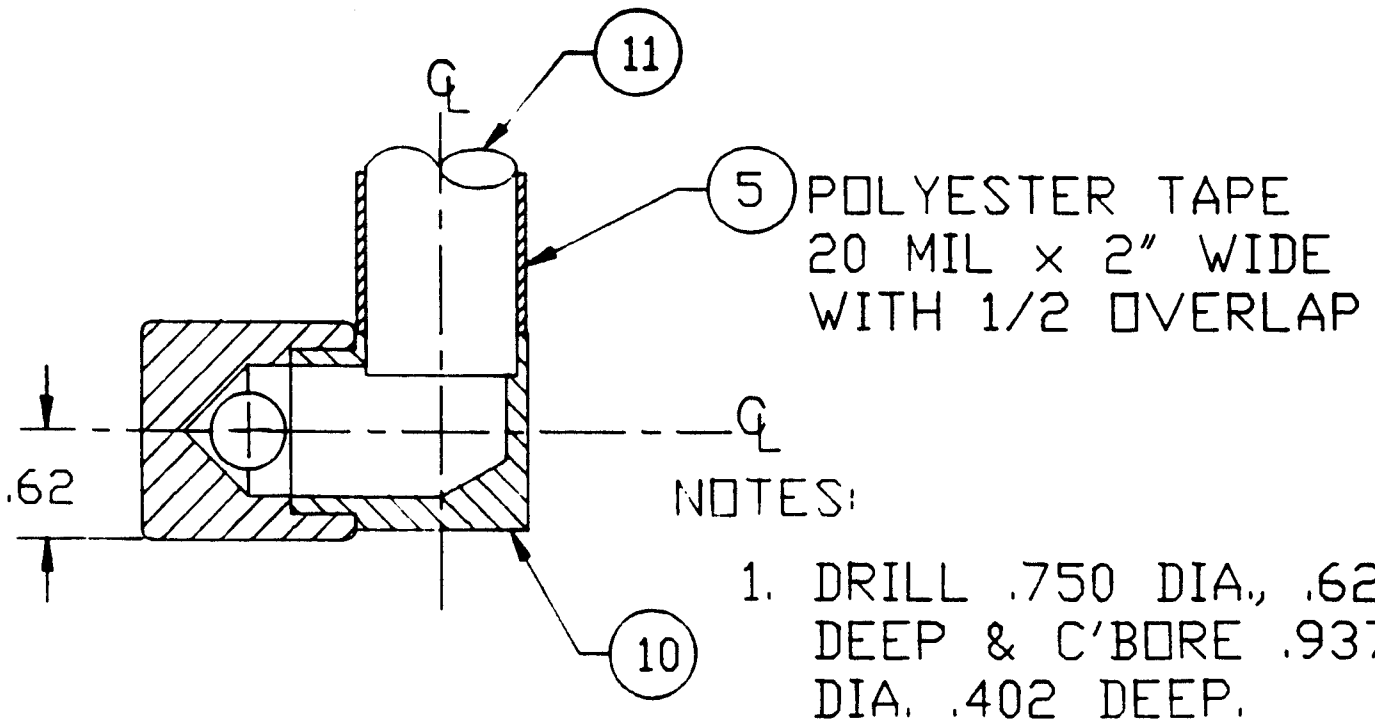


Figure 2 CDIF Conductor Cross Section
(dimensions in inches)



DETAIL F

SCALE: 1=1

TYPICAL WATER FITTING

Figure 3 CDIF Conductor Cross Section (from MSE redrawing of
MCA Drawing E-3112, Rev G, 1/5/80)

A few of the temperature switch circuits have failed to a permanent open circuit condition and are no longer monitored at all. Instead of relying on the temperature switch for an over-temperature condition in the corresponding water circuit, voltage taps on the related water circuits are monitored periodically during a magnet run by plugging a portable DVM into the appropriate banana jacks on the temperature status panel. The DVM reading must be compared with a graph which plots voltage vs. magnet current for both 60° C and 90° C copper temperatures. Operation is not allowed for voltages above the curve on the plot corresponding to copper resistance in the magnet water circuit at 90° C. If the operator measures excessive voltage at these jacks during a run, he is again obligated to communicate the need for an emergency magnet shutdown. Since each water circuit has a different length, each circuit monitored in this fashion has its own shutdown curve which must be interpreted by the operator after he has entered the appropriate curve with the measured voltage and the operating current. There are currently two such water circuits in each of the East and West coils, giving a total of 4 DVM measurements which must be made periodically during any magnet run.

2.1.2 Failure Discovery

In February 1991, a problem in the MHD channel developed during a run, and an emergency shutdown ensued. Prior to accessing the channel for service, the crossover bus bar was deliberately grounded as a safety precaution. Upon grounding the winding, a control power fuse blew and another temperature switch contact short to the coil was suspected. Upon further investigation the following was discovered:

- 1) Low megger and resistance readings on the West coil to ground, even after draining water from the magnet
- 2) An additional temperature switch which was shorted to the coil
- 3) Water leaking from the West coil end-turn region

In order to locate the source of the water leak, each of the double pancakes of both East and West coil halves were hydrostatically tested using N₂ gas. Each double pancake was sealed after pressurization to about 275 psig, and pressure was monitored over time. The only significant leak found was in the number 2 pancake in the West coil, which showed a pressure loss rate of about 5 psi/min. Leak test results for the 6 double pancake windings of the West side coil are shown in Figure 4 (courtesy MSE). During the test on the number 2 double pancake, gas could be felt exiting from the inside vertical surface that faces the magnet iron in the end-turn region. Bubble solution sprayed over the end-turn surface also revealed a gas leak in the vicinity of the leads to the temperature switches which are mounted on double pancakes 2 and 3. Isolating the leak within the number 2 double pancake to one of the 90 water fittings was eventually achieved by a fill-to-a-level-and-pressurize routine and subsequently verified by borescope.

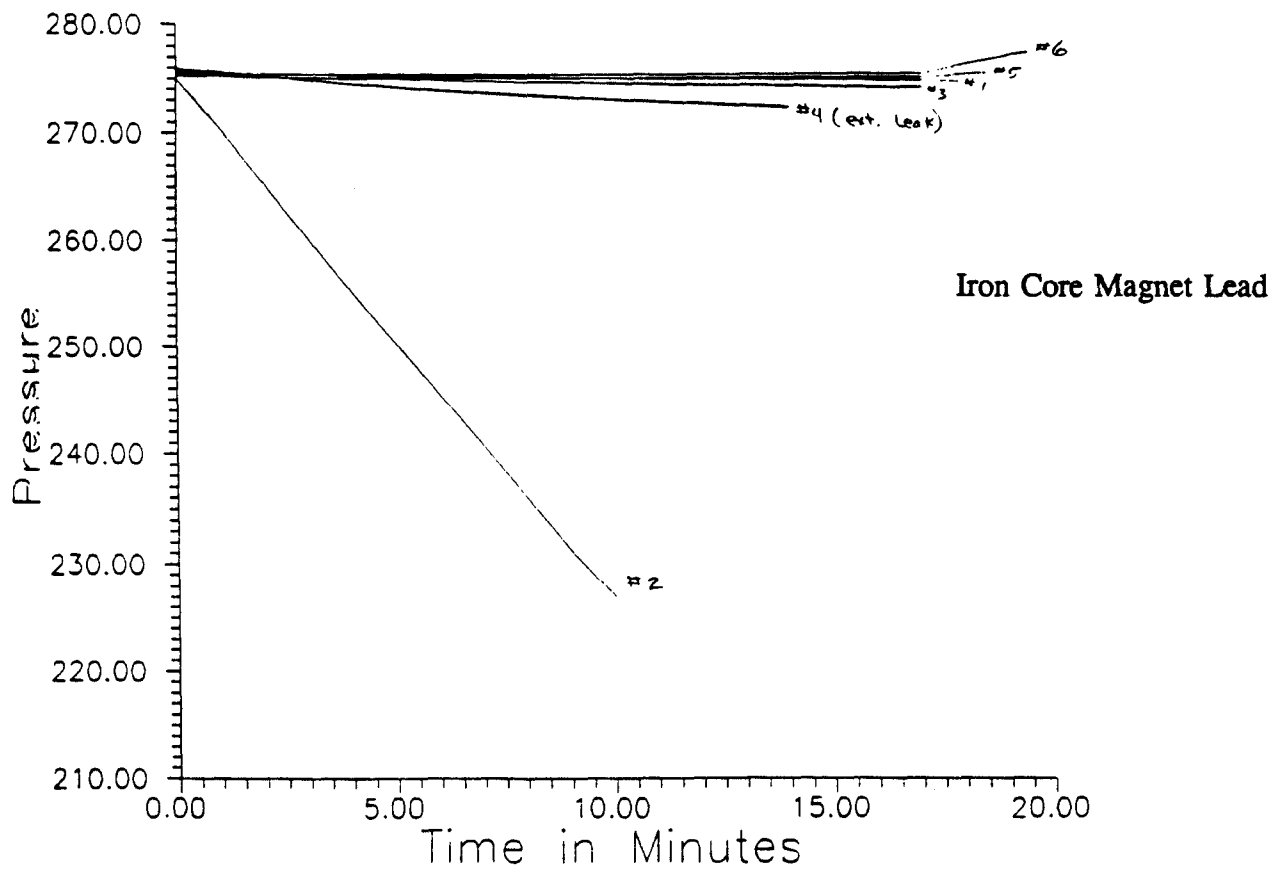


Figure 4 Hydrostatic N₂ Pressure Test in Double Pancakes 1-6
(courtesy MSE)

2.1.3 Other Items Noted During Evaluation

At some time since the installation of the magnet, some of the water hoses were replaced with hoses having iron rather than stainless fittings which were provided on the original equipment hoses. The iron fittings are subject to rather severe corrosive action, with the buildup of scale so great that significant blockage of the water flow resulted. None of the iron fittings, however, were on hoses connected to the number 2 double pancake in the West coil where the water leak developed.

Another item of interest was whether there had been any degradation of the heat transfer coefficient from the copper to the cooling water channel over time due to fouling of the wall. To evaluate this possibility, the derived heat transfer coefficient was plotted as a function of cooling water flow rate using data from the original acceptance test [4] and compared with data from a recent run on 2/7/91. This comparison is presented in Figure 5. The plotted data, together with transcriptions of the acceptance test and 2/7/91 data are tabulated in the accompanying tables. The data from the recent run on 2/7/91 shows heat transfer coefficient values outside the scatter band of the acceptance test data. The heat transfer coefficient in the recent data is still in the vicinity of $6000 \text{ W/m}^2 \text{ C}$ at full field, but about 550 gpm of cooling water flow are now required to maintain that heat transfer coefficient, whereas at the time of acceptance testing, only about 400 gpm were required to maintain the same heat transfer coefficient. Additional recent data in the 200-400 gpm range would be useful to fully assess the degradation.

The original design was based on a flow control requirement to maintain a constant average copper temperature. With this control approach, the magnet has maintained a constant operating temperature in spite of a degrading heat transfer coefficient. If, however, the heat transfer coefficient continues to degrade with time, some limit to the water pumping power will be reached unless measures are taken to clean the wall of the cooling channels.

2.1.4 Recommendations from Evaluation

After the evaluation of the failure, the following recommendations were made:

- 1) Hydraulically isolate and electrically jumper around the failed double pancake rather than attempt to seal the leak.
- 2) Create a new interlocking function based on an automatic over-temperature trip derived from a calculation of the temperature of each cooling circuit based on that circuit's electrical resistance. These resistances, and in turn, the temperatures, would be derived from the voltage tap and current measurements. In conjunction with this change, the voltage tap wiring should be rerun so each tap wire is twisted with each other in each magnet half, and only at the point of connection should the individual wire be separated from the twisted bundle. This will minimize inductive pickup during current ramping. This approach is recommended as an addition to, rather than in place of, the temperature

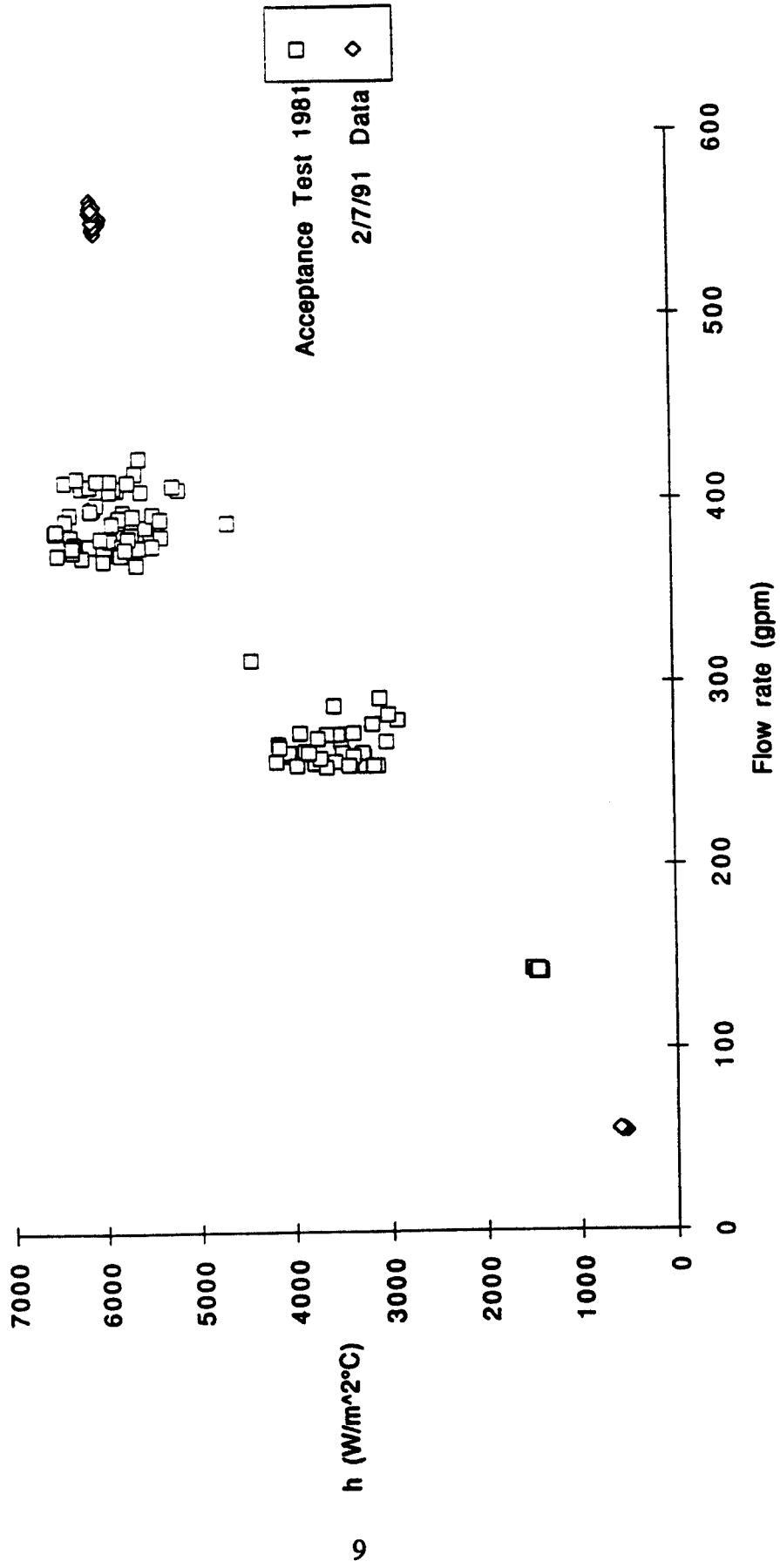


Figure 5 CDIF ICM Heat Transfer Coefficient vs. Flow Rate Comparison--Acceptance Test vs. Recent Data

switch system now in effect. If this resistance-temperature-correlated interlock is adopted, the cumbersome procedure of manually monitoring the 4 voltage tap circuits in which the temperature switches have failed may be circumvented.

CAUTIONARY NOTE

A real concern is that if a temperature switch has both of its contacts shorted to magnet copper, or if the switch is now constrained in a position by the copper winding so it cannot open, there is no way to tell this condition from the normally closed state of the switch contacts. There could be some switches in this condition already if several are known to have failed by shorting at least one contact to magnet copper. If there are switches with both contacts shorted, they cannot provide the intended over-temperature protection. For this reason, it is mandatory to invoke the voltage-tap-based interlock system.

- 3) Install a ground fault detection system which should detect ground faults and initiate automatic magnet shutdown more reliably than the loss of 120 Vac control power does now.
- 4) Examine all recent voltage tap data and look for any indication of local overheating in any of the hydraulic circuits. If any of the circuits appear to be overheating, do not return to power until the situation is thoroughly understood, and the problem is isolated.
- 5) Remeasure flow rates in all the individual water circuits of both magnet halves (except in West #2 pancake) and compare with acceptance test data to ensure there are no flow restrictions which might lead to over-temperature conditions.
- 6) With the West #2 pancake still in the circuit, rerun a magnetic field profile for the magnet at 500 amperes and compare results with data taken and recorded in the Acceptance Test Report. Adiabatic calculations indicate that 500 A can flow through the windings without cooling for up to 3 hours, if required. The interlocking function of 1) above should be fully debugged and operational prior to running the field check. Temperatures should not be allowed to rise more than 20° C above room temperature. This provides a safety factor of 2 on temperature rise with respect to normal operation. Any changes in magnetic field at the same current could be indicative of internal shorts in the magnet.
- 7) Thoroughly bake out the coil using the standard preheat procedure. Periodically check 500 V megger readings to ground, and discontinue baking only after these megger readings have reached their prefailure levels.
- 8) Invoke slower current ramping times. This will minimize inductive pickup in the voltage tap wiring, and prevent false trips. The appropriate ramp rate will have to be determined experimentally.

- 9) Pursue cleanup of the cooling channel walls in an effort to restore the original heat transfer coefficient of about $6000 \text{ W/m}^2 \text{ C}$ at 400 gpm.

For the longer term, replacement coils should be ordered while there is still some life remaining in the existing magnet.

2.1.5 Present Magnet Status

The leak in the number 2 double pancake was repaired with a metal sealant by National Nuclear Corporation, Ltd. The repair has been successfully pressure tested. As a backup, an electrical jumper has been designed for jumpering from the number 1 to the number 3 double pancake. With the jumper connected, the magnet may be operated on eleven out of twelve of the double pancakes, and the number 2 double pancake would be hydraulically isolated.

As of this writing, the magnet was recently operated to above 6000 A. With the magnet running at less than full field on all twelve double pancakes on 12/19/91, the magnet had to be shut down for other reasons. Following shutdown, it was discovered that the magnet is leaking water in the vicinity of the previous leak in the number 2 double pancake. Details as to the exact location of the leak are under investigation at this time.

2.2 TEXT Tokamak

2.2.1 Coil Design

The elevation view of the coil layout on the TEXT Tokamak is shown in Figure 6 (courtesy of TEXT). An iron frame returns the flux of the poloidal field coils. The poloidal coils consist of the Ohmic Heating (OH), Divertor (DIV) and Vertical Field (VF) coils, which are all wound as semicircular ring segments and are installed inside the bore of the TF coil. The coil conductor material is an alumina-dispersion-strengthened (ADS) copper (C157 series). The semicircular turn segments of the coils are joined by finger joints which are positioned, insulated and clamped together during machine assembly in rather tight working quarters. Visual inspection of the joints is made possible in some locations only by the use of small mirrors. The "divertor" winding bundle comprises four turns, in a 2×2 array, redundantly labeled the "divertor" winding, and four additional turns in another 2×2 array, labeled the "bias" winding. Under certain modes of operation, the divertor and bias windings are not energized, but voltages may nevertheless be induced in these windings in the presence of transient poloidal fields. Because of the manner in which the turns are wound and connected, the worst case voltage between the divertor and bias windings is three turn-to-turn voltages.

Figure 7 is a sketch of the finger joint region where the turns of the divertor and bias windings lie adjacent to each. It is the relative placement of the composite mica and the Nomex paper insulations during joint assembly that is both most critical and most difficult due to cramped working space and poor visibility.

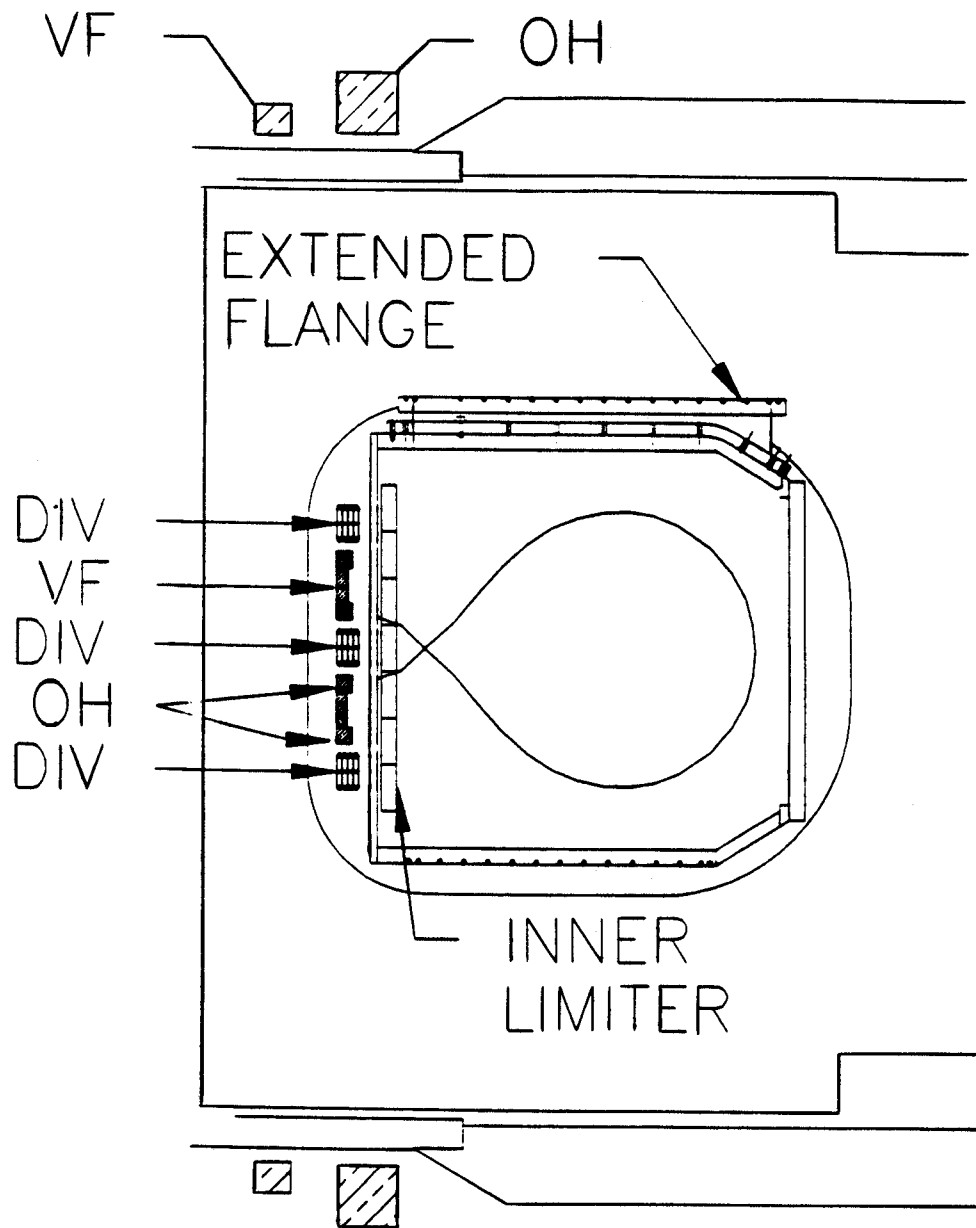


Figure 6 Partial Elevation View of Text Machine (courtesy TEXT Project)

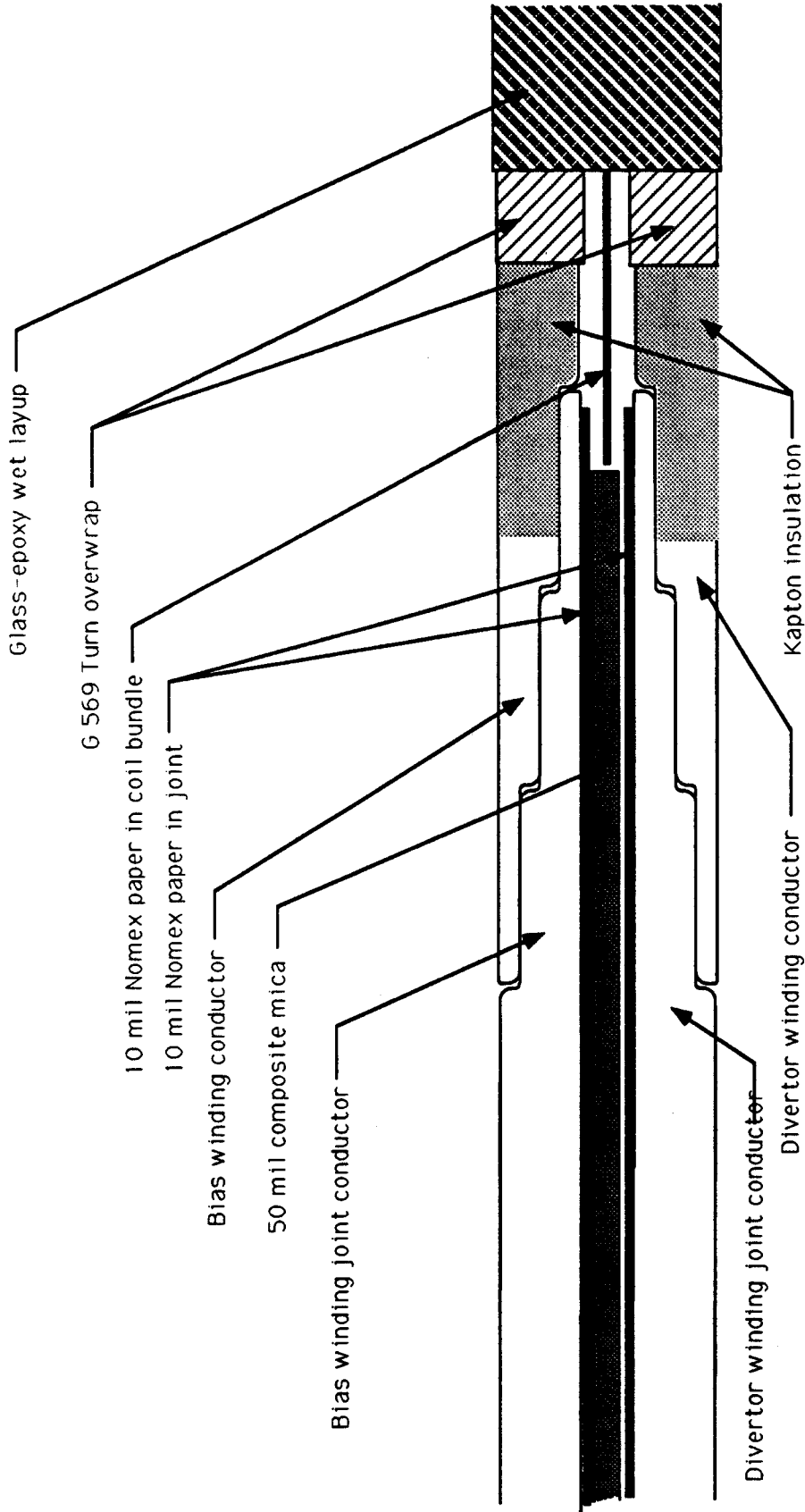


Figure 7 Insulation in Region of Failure

Prior to installation of the joint links, both the turn-to-turn and the winding-to-winding insulation were tested to 2500 Vdc. After the joint links were installed, the coil was tested with over 1200 10 kA, 200 ms pulses and then the joint clamp bolts were retorqued.

Crowbar protection in the OH circuit is shown in Figure 8 (courtesy TEXT). During a plasma disruption, voltage is induced in the OH coil due to changing plasma current and/or position. When the current in the 200 μ F capacitor exceeds 400 A, the ignitron fires and shorts the OH coil through an 0.12 ohm resistor, thereby limiting the OH voltage to safe levels. During loop voltage testing outside the vacuum vessel using a digitizer with a 10 kHz sampling rate, no voltage was found greater than 85 V.

2.2.2 Failure Discovery

During an increase of the plasma current from 150-175 kA to 200 kA, and while the divertor/bias windings were not energized, the plasma became very disruptive and the sound of the shots changed. Upon investigation, flashover was noted in the vicinity of the lower divertor-bias winding. Insulation in the failed region was burned away and the joint and coil fingers were coated with carbon/ash.

2.2.3 Failure Evaluation

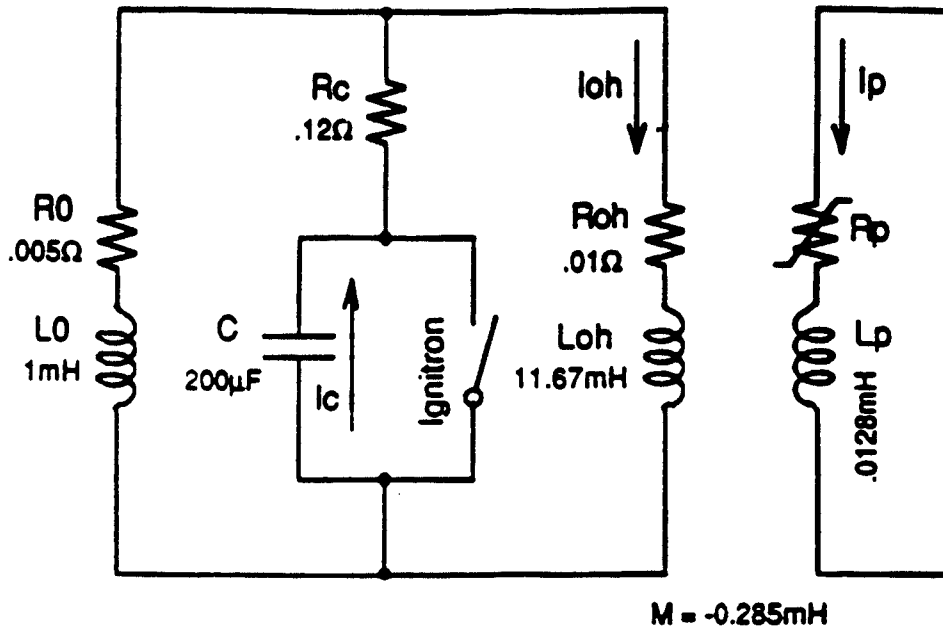
Photographs taken in the region of the flashover prior to joint disassembly showed what appeared to be about 1/2 inch of insulation overlap between the coil and joint Nomex paper insulations. This observation lead to two considered possibilities: 1) a metal chip or other foreign debris was present in the joint region which compromised the insulation integrity, and 2) the loop voltage may have been greater than the design value.

The presence of foreign material in the joint region remains a possibility which cannot be confirmed due to the damaged condition of the entire region following the flashover.

To evaluate the loop voltage, a simple circuit analysis was performed on the circuit components shown in Figure 8 (i.e., no vacuum vessel and no other coil reactions). Assuming a plasma decay rate of 50 MA/s and a coupling coefficient of 0.8 between the plasma and the OH coil, the 40 turn OH coil voltage rises to about 77 V per turn in the first 8 microseconds, the time it takes the ignitron to fire. Then the OH voltage drops to about 60 V/turn immediately after the ignitron fires, and eventually decays to zero (assuming the OH source has, by then, been shut off). Thus, based on the simple analysis, it appears that there are indeed no fast voltage peaks and 85 volts appears to be a reasonable turn-to-turn maximum, provided the ignitron fires.

If the ignitron does not fire, circuit analysis indicates that the OH voltage can rise to a value in excess of 40 kV, with the first peak occurring at about 0.5 ms. The 40+ kV would put 1000 V/turn on the OH coil and 43 V/mil across the bias-to divertor winding insulation. This voltage stress would not break down the winding-to-winding insulation (if it were defect free), but would be sufficient to cause it to surface track if a surface tracking path existed. Whether

- 1.) Simulation model of the protective circuit for the disruption.
Only consider the plasma and oh circuits.



- 2.) Initial conditions:

- $I_{\text{plasma}}(0) = 400\text{KA}$.
- $I_{\text{oh}}(0) = 10\text{KA}$.
- $V_{\text{oh}}(0) = 100\text{V}$.

- 3.) Calculate conditions :

- The plasma current decay for the disruption is 50 MA/Sec.
 - The largest loop voltage of plasma is about 250V.
 - The ignitron be fired, if $I_c > 400\text{A}$.
 - The time delay of protective system is about 8 μS .
- Assume the impedance of the oh power source : $R_0 = 0.005\Omega$, $L_0 = 1\text{mH}$.

Figure 8 OH Protection Circuit and Parameters (courtesy TEXT Project)

the voltage could ever reach 40 kV is questionable, as the 200 μ F capacitor would probably break down well below this level.

2.2.4 Recommendations from Evaluation

- 1) The ignitron firing reliability should be determined by testing under conditions which duplicate disruption as accurately as possible.
- 2) The output of the power supply used during the 1200 divertor shots should be checked for voltage spikes using a high frequency scope under similar conditions of inductive load and current level.
- 3) Since Nomex paper is noticeably porous, two 5-mil layers would be much better than one 10 mil layer in all locations.
- 4) If there is any slippage at the clamped joint, the possibility exists for making conductive dust in the region. The TEXT staff advised that the friction of the plated surfaces together with the clamping force were sufficient to ensure no slippage. This condition should be verified for disruption loads as well as normal operation.
- 5) A more detailed analysis of the loop voltage was suggested.
- 6) The rebuild of the failed coil should begin with bare conductor, rather than attempting to cut out and patch the bad insulation. Beginning with bare conductor and reinsulating is the only way to ensure that all of the old insulation defects are removed.
- 7) Temperature ratings of all materials should be double checked. One of the analyses (reference b) shows that the joint temperature can rise to 150 - 200° C.
- 8) Teflon spacers should be employed to preserve space for overlap of the joint Nomex cuffs on both sides of the Nomex paper in the coil bundle ends during epoxy cure.
- 9) Add a specification for corner radii on all corners in the joint region, and add a quality inspection for these.
- 10) Steps ensuring proper cleanliness during the rework cannot be overemphasized.
- 11) Add a capacitive ring test to check the turn-to-turn insulation both before and after installation of the joint links.

2.2.5 Present Coil Status

A redesign of all of the inner poloidal field coils is in process. The new design concept is for a single-turn-width stack for each of the coil bundles, with the joints being welded, rather

than mechanical, and using Chrome Copper 182 as the conductor material, rather than the ADS copper, which is not easily welded, if at all. An extensive testing program is underway to determine the mechanical strength of the welded joint using chrome-copper filler rod with TIG weld procedures. A concern for welding in the vicinity of electrical insulation must be carefully addressed. Design review of the new concept is scheduled for December 1991.

2.3 ATF Stellarator

2.3.1 Coil Design

The Advanced Toroidal Facility was constructed in the mid-to-late 1980's and is shown in Figure 9 (courtesy ORNL). The two intertwined helical field (HF) coils are fabricated from multiple identical copper segments which are electrically connected via clamped finger joints, three turns of which are shown schematically in Figure 10. Because of the open nature of the machine, the bare conductors in these joints are exposed directly to the atmosphere. The coils are designed to produce a full field of 2 T, although many physics shots have been conducted at the 1 T level. On full-field shots, the HF coils are ramped up to 120,000 A in 2 s with a power supply voltage of 1300 V. During the 1300 V ramping, the turn-to-turn voltage on the HF coils is nominally 325 V. The ramp-up timing is coordinated with powering the outer, followed by the inner vertical field coils.

2.3.2 Failure Discovery

In May of 1991, the first 2 tesla shot was fired since a single 2 tesla shot had been fired two months earlier. The HF power supply was turned on and applied normal voltage to the HF coils. The outer and inner vertical field coils were then powered in sequence. At that time a loud shotgun-like sound was heard throughout the facility, and the operator observed arcing on the TV monitor [3]. Upon disassembly, there were indications of several turn-to-turn faults within one of the HF coil segments, and severe damage to at least two of the 24 segments was sustained. Significant amounts of copper were melted from the conductors in the region of the failure. With this failure, far more than in the previous two, one quickly gains an appreciation of how destructive the energy stored in these large magnetic fields can be if this energy is allowed to dump, even in part, into a localized area of the winding.

2.3.3 Failure Evaluation

Because there had been many previously successful shots at the full field level, the initial design appears to have been adequate, but during the time from the last successful shot at 2 T in March 1991 and the May incident, something had to have changed. In reviewing the operating history, the sequence of events and conditions identified below may be significant:

- 1) A set of error coils was installed 180° apart in March 1991. One of these was located above HF coil segment 17, where the failure occurred. Both of the error coils had experienced water leaks, the last one above segment 17 on March 20. The

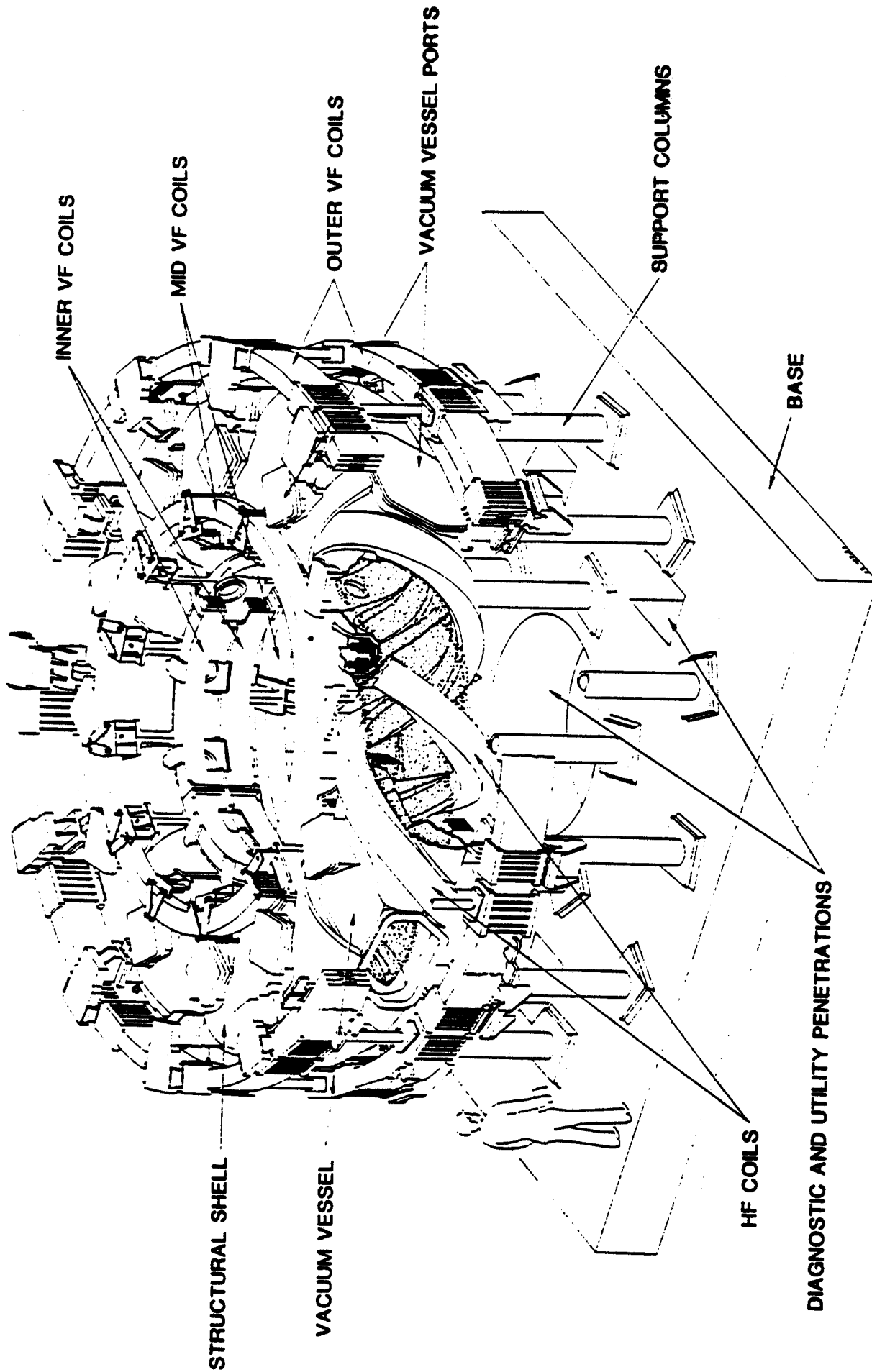


Figure 9 Advanced Toroidal Facility at ORNL (courtesy ATF Project)

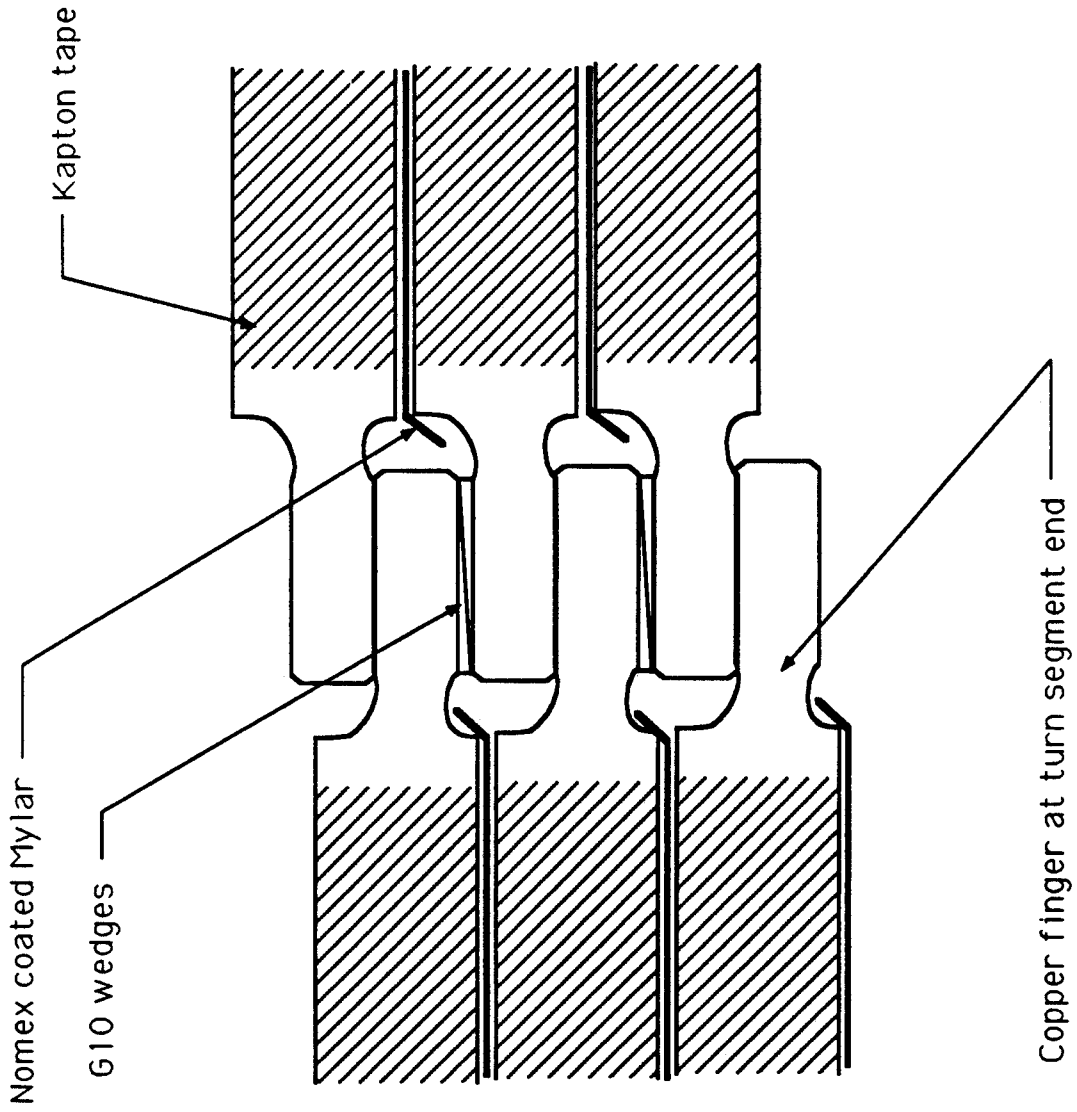


Figure 10 Three-joint Section of ATF Joint Region Showing Present Design

visible/accessible water from these leaks was sponged up, and the areas were warmed with a heat gun.

- 2) The last successful shot at 2 T was made on March 21, 1991.
- 3) On March 22, 1991, part of a burned hose fitting from the error coil above segment 17 was found on the floor at the base of the ATF. Evidence was found that a flashover had occurred between an unused fitting on the error coil and the coil's power supply bus.
- 4) The timing for energizing one of the vertical field coils during the shot in which the accident occurred was not correct. This timing error could have induced transient voltages, although no direct link between the timing error and the failure has been established.
- 5) There is no single point ground reference in the system.
- 6) There is no procedure at present to perform a turn-to-turn voltage test as a part of routine maintenance. Coil ringing tests are not performed, and dc testing had been considered impractical due to the time required to disassemble a coil joint.
- 7) The exposure of bare copper in the joint region to the atmosphere (and water, dust, debris from nearby flashovers, etc.) makes it a likely failure region.

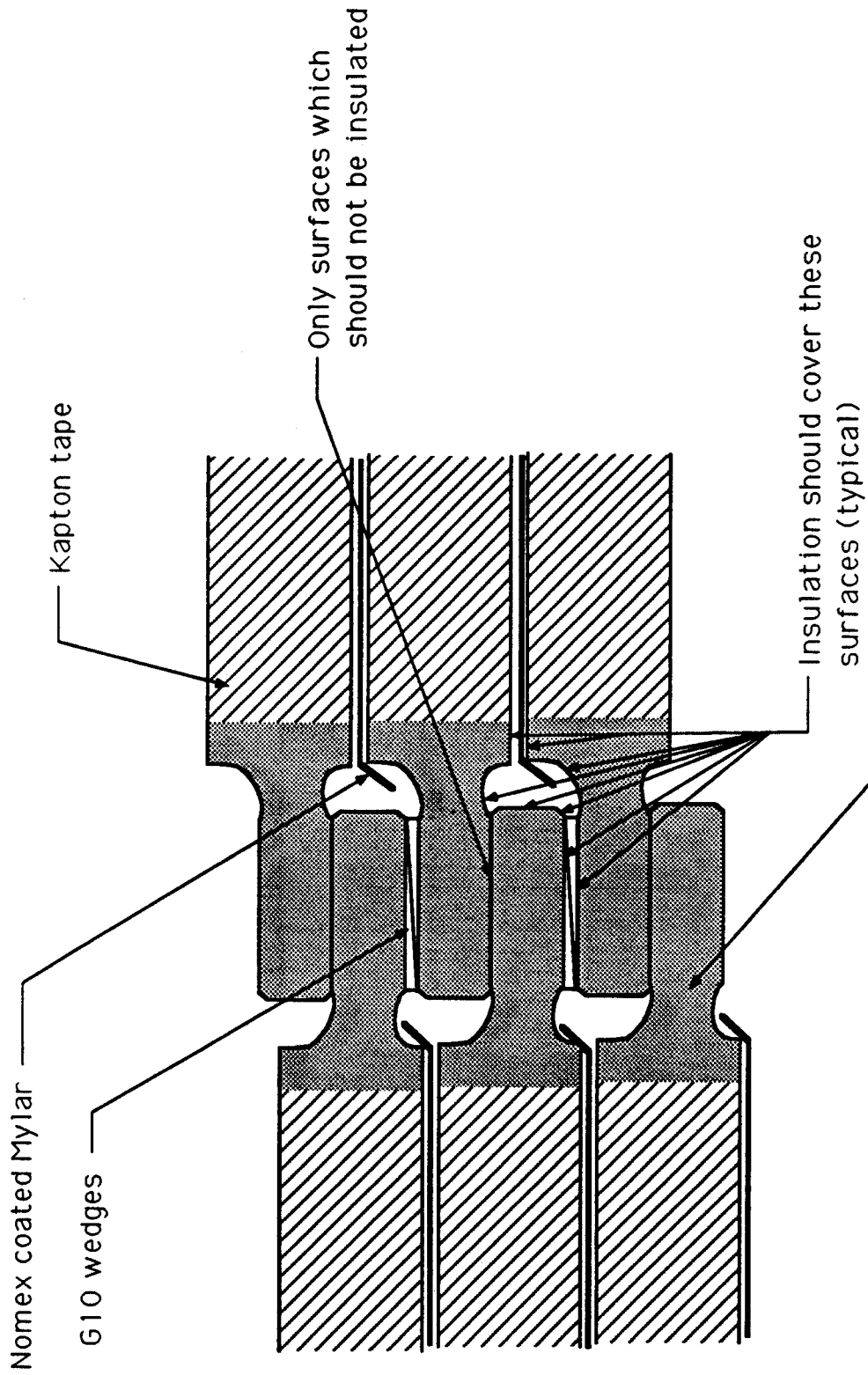
2.3.4 Recommendations from Evaluation

Recommendations include the following:

- 1) Establish routine preventive maintenance checks of the turn-to-turn insulation integrity.
- 2) Establish more effective drying routines following water spills or leaks.
- 3) Provide additional insulation on the exposed joint surfaces as shown in Figure 11.

2.3.5 Present Magnet Status

The carbon-tracked joint regions were cleaned and an insulating, epoxy-based paint was applied to cover the exposed conductor surfaces as a temporary repair. This enabled a few additional shots at reduced duty cycle prior to beginning a complete machine disassembly, which is underway now.



Surfaces which are bare now and could be insulated (eg., by extending the Kapton tape, or using an insulating paint)

Figure 11 Three-joint Section of ATF Joint Region Showing Areas of Exposed Copper that Could be Insulated

References

1. P.H. Edmonds, et al., "TEXT Upgrade Description & Status," presented at 32nd Annual Meeting, Division of Plasma Physics, APS, November 12-16, 1990.
2. Investigation of Helical Field (HF) Coil Joint Fault on the Advanced Toroidal Facility (ATF)," Interim report of the ATF Investigative Team, June 1991.
3. Mosko, Sig, "The ORNL ATF Coil Accident 5/30/91," Draft of Technical Notes dated 6/26/91.
4. Magnetic Corporation of America, Final Acceptance Test Report, CDIF Conventional Magnet, Model WCM-3, September 1981.
5. Magnetic Corporation of America, Technical Manual, CDIF Conventional Magnet, Model WCM-3, Volume 1, Revision A, January 1980.

3.0 Quench Code Development

3.1 HESTAB and CICC Capabilities

HESTAB is a zero-dimensional stability code for analysis of cable-in-conduit conductors [1, 2]. The main assumption of the 0-D model is the axial length independency of the problem, which would hold for low induced helium velocities in the early stages of the recovery process. Figure 12 shows the system under consideration, which is composed of the conductor and supercritical helium.

The 0-D model requires the solution of the energy equations for the conductor (copper and superconductor) and for the helium. In solving the zero-dimensional helium energy equation it should be noted that the helium density is also an unknown. Thus to close the system of equations it is necessary to include the continuity, momentum and state equations of the helium. In accordance with the 0-D model HESTAB assumes the helium density to be a constant (low helium velocity assumption).

CICC is a one-dimensional quench code that models forced flow helium cooled conductors as shown in Figure 13. The relevant equations solved by the code are documented in references [1, 3, 4]. In solving the 1-D model, the accuracy of the results and the CPU time are dependent on the chosen method of solution. Extensive CPU time on the Cray is required in quench simulations performed by CICC (the required CPU time on the Cray is about 6000 times longer than the real simulation time). Although this time multiplier may be acceptable in calculating whether or not a configuration is stable, it is the driving factor in the need for development of a fast code for quench simulation since the latter occurs on time scales which are orders of magnitude longer than those required to determine whether or not a configuration is stable.

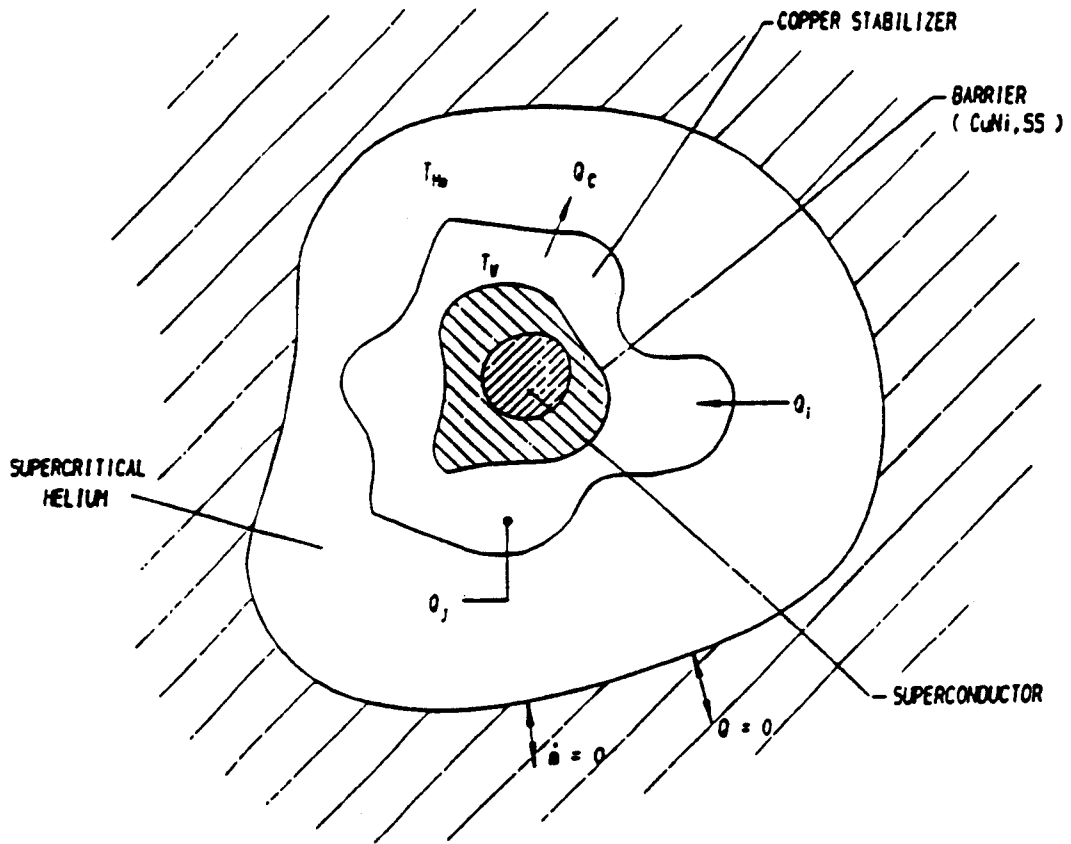


Figure 12: Cable-In-Conduit Schematic Modeled by HESTAB (from Reference [1]).

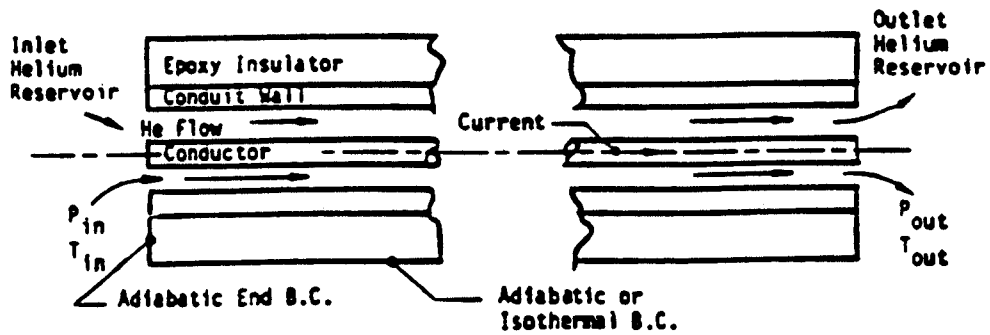


Figure 13: Cable-In-Conduit Schematic Modeled by CICC (from Reference [1]).

3.2 Comparison with Bus Data

During FY90-91, the MIT PFC was responsible for the design and construction of the stabilized power buses for the Superconducting Super Collider full-scale prototype dipoles. As part of this activity, we constructed a subscale model of the bus which operates in supercritical helium and has many features found in typical ICCS conductor configurations. The experiments verified the required bus performance. Some of the data and a description of the bus configuration can be found in Thome, et al. [5]. The data generated in the bus program are available for our use in evaluating and constructing codes for stability and quench propagation in ICCS types of conductors.

Figure 14 shows a typical result for data taken to determine energy margin for the bus compared with computed curves using HESTAB. The energy margin is the maximum amount of energy input to a conductor without causing an uncontrollable propagating normal zone. It is a direct measure of the stability of the configuration. The parameter, λ , for the computed curves is the assumed fraction of exposed conductor surface within the configuration. As indicated, the code HESTAB, which is relatively efficient, gives a reasonable match to the measured values over the midrange of the operating current, which is the most likely area for design. Comparisons using the code CICC to calculate energy margin were similar.

HESTAB, as mentioned earlier, is a zero-dimensional code, and is not appropriate for computation of quench characteristics. As a result, comparisons were made using the code CICC. These were found to be unreliable and, as a result are not presented here. In addition, the runs were extremely time consuming for prediction of quench behavior, in particular, the form of the conductor voltage transient as the quench progressed. This may be attributable to the more complex geometry and flow paths in the bus configuration when compared to more conventional ICCS conductors (single flow path) in which the one-dimensional model assumed by CICC may be more reliable.

As a result of the above, we are pursuing development of a quench code with the goal of improved speed for prediction of quench characteristics, but with the flexibility to allow treatment of conductors with the multiple flow paths which are characteristic of the SSC bus design or of the US/Japan DPC coil. [6]

3.3 Future Work

The inability to obtain reasonable agreement between the one-dimensional models in CICC with the multiple flow path type of conductors in the SSC bus or in the US/Japan DPC coil have led us to the need to improve the models as well as increase the speed of the codes for analysis of quench.

The design of the SSC bus and of the US/Japan DPC conductor consists of two distinct helium flow paths. One path is through the conductor and the braid, and a second channel is present on the sides of the braids or in an adjacent channel. The helium behavior (cooling

Energy Margin vs. Current

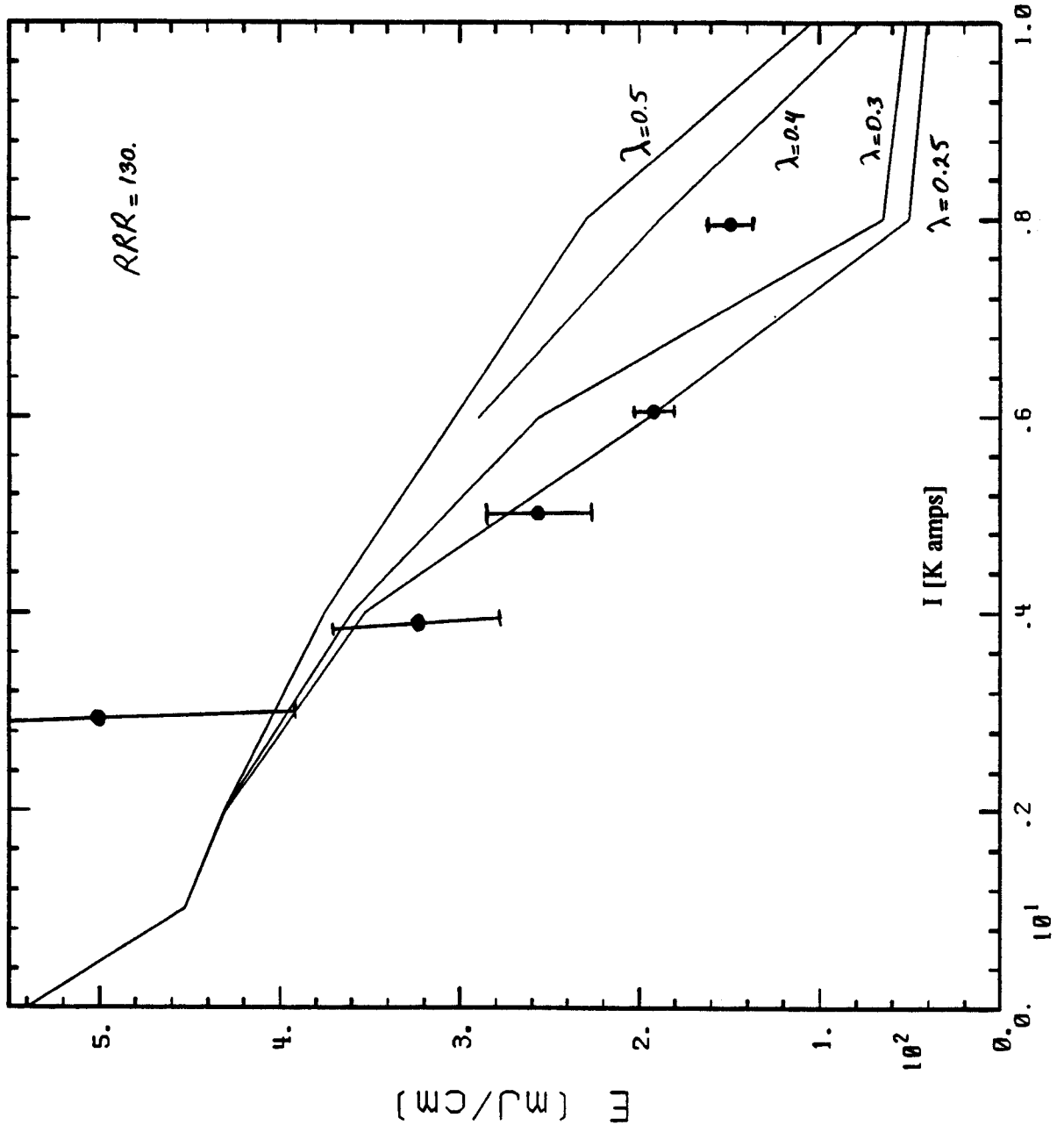


Figure 14 Comparison of Measured and Computed Values of Energy Margin for the SSC Dipole Bus; λ = Fraction of Cable Wetted Perimeter

capabilities) is different in each of these channels and requires solving the one-dimensional mass, momentum, and energy equations for the helium in each additional channel which allows heat flow between the channels. This will be modeled in the new code.

In addition, the new code will allow for more complex boundary conditions. CICC models the boundary conditions at the ends of the channel by assuming the presence of an infinite reservoir at these boundaries and, as a result, constant pressure. In the experiments performed on the bus, there is a finite reservoir present at the ends of the channel. A pressure rise as high as 50% is observed to occur in the finite reservoir. Such a pressure rise at the axial boundaries of the system give rise to different helium flow characteristics that must be modeled.

By including a more physical model the new code should be more accurate in predicting the experimental measurements. It is also intended to develop the code in such a way as to be much faster than the existing one dimensional codes. In simulations that were performed in analyzing the experimental results, it was found that the typical CPU time used by CICC in a 4-second quench simulation is about 2-6 Cray-hours. It is apparent that in order to perform parametric studies of new superconducting magnet designs faster tools are required. The objective of the new code is to allow for parametric studies to be performed on a Vax-Station or PC.

References

- [1] Thome, R. J., "Safety and Protection for Large-Scale Magnet Systems - FY 90 Report," PFC/RR-91-1, January 1991.
- [2] Minervini, J. V. and Bottura, L., "Modeling of Transient Stability in Cable-in-Conduit Superconductors," personal communication (to be published), The NET Team, 1990.
- [3] Wong, R. L., "Program CICC, Flow and Heat Transfer in Cable-in-Conduit Conductors-Equations & Verification," Lawrence Livermore National Laboratory Internal Report, UCID 21733, May 1989.
- [4] Wong, R. L., "Program CICC, Flow and Heat Transfer in Cable-in-Conduit Conductors-User's Manual," Lawrence Livermore National Laboratory Internal Report, UCID 21941, February 1990.
- [5] Thome, R. J., Hale, R. J., Montgomery, D. B., et al., "Bus Design, Development and Test for the Superconducting Super Collider," presented at MT-12, Leningrad, June 1991 (to be published).
- [6] Painter, T. A., et al., "Test Data from the US-Demonstration Poloidal Coil Experiment," PFC/RR-92-1, January 1992.